Inorganic Chemistry
Article

Inorg. Chem. **2010**, *49*, 2267–2272 **2267**
DOI: 10.1021/ic902065q

Temperature-Dependent Synthetic Routes to and Thermochemical Ranking of α- and β-SrNCN

Michael Krings,[†] Michael Wessel,[†] Wolfgang Wilsmann,[‡] Paul Müller,[†] and Richard Dronskowski*[,†]

[†]*Institut für Anorganische Chemie and* [‡]*Institut für Gesteinshüttenkunde, RWTH Aachen University,*
52056 Aachen, Germany

Received October 19, 2009

White powdery β-SrNCN was obtained by the solid-state metathesis between SrI_2 and ZnNCN at 843 K, by the reaction of SrI_2, CsCN, and CsN_3 in tantalum cylinders at the same temperature, and from the direct reaction between elemental Sr and H_2NCN dissolved in liquid ammonia. The solid-state reactions carried out at a higher 973 K yield white α-SrNCN. Both experimental data (X-ray diffraction (XRD), infrared spectroscopy, differential scanning calorimetry (DSC)) as well as GGA density-functional phonon calculations show that the β-phase is thermochemically more stable, by a minute 2 kJ/mol (electronic-structure theory) and about 6 kJ/mol (DSC), whereas the α-phase is slightly more dense. In addition, both XRD and DSC measurements reveal two distinct (endothermic) steps for the β-to-α phase transition, that is, first around 920 ± 20 K, then at 985 ± 15 K based on the X-ray data. Thermochemically, the upper heat effect is larger by a factor of 20.

Introduction

As a fundamental class of compounds in the fields of solid-state and also molecular chemistry, cyanamides and carbodiimides have gained increasing attention within the past decade. Because of their −2 anionic charge, both cyanamide and carbodiimide structural units allow the realization of a nitrogen-based pseudo-oxide chemistry since NCN^{2-} and O^{2-} are isolobal entities; thus, NCN^{2-} is able to replace O^{2-} in several novel materials. A number of alkali metal,[1] alkaline-earth metal,[2] transition-metal,[3-6] and main-group metal[7,8] cyanamides as well as carbodiimides were obtained following different synthetic routes.

With respect to the alkaline-earth carbodiimides, the crystal structure of strontium carbodiimide, α-SrNCN, was first reported by Strid and Vannerberg[9] already more than 4 decades ago. They obtained this particular phase by the reaction of $SrCO_3$ with HCN at temperatures between 773 and 973 K. At the beginning of the 21st century, an alternative phase, dubbed β-SrNCN, was first synthesized by Wissmann using a reaction between $SrCO_3$ and flowing NH_3.[10] The temperature dependence of that particular reaction is striking: at 873 K, β-SrNCN is obtained whereas, at 1173 K, the same reaction yields α-SrNCN. Interestingly enough, and also a bit counterintuitive, the low-temperature but high-symmetry ($R\overline{3}m$) β-phase was estimated by primitive Madelung lattice-energy calculations as being *metastable* by about 9 kJ/mol if compared with the high-temperature but low-symmetry (*Pnma*) and presumably stable α-phase. There is no simple explanation for that obvious contradiction, but we note that Wissmann highlights that β-SrNCN can only be synthesized by starting with high-surface $SrCO_3$. Thus, it is not fully clear at the outset whether α- or β-SrNCN is the stable carbodiimide phase.

Figure 1 reveals the crystal structures of both polymorphs of SrNCN. In both phases, Sr^{2+} is octahedrally coordinated by nitrogen atoms from the $N{=}C{=}N^{2-}$ carbodiimide groups, and one finds C═N double bonds of about 1.23−1.24 Å in both. The only structural difference, however, is given by the *orientation* of the carbodiimide groups. Within hexagonal β-SrNCN, all six NCN^{2-} units are arranged parallel to each other along the *c* axis such that the edge-sharing octahedra form "layers" within *ab* which are separated by the carbodiimide units. In the orthorhombic crystal structure of α-SrNCN, however, four carbodiimide units lie parallel,

---

*To whom correspondence should be addressed. E-mail: drons@HAL9000.ac.rwth-aachen.de. Fax: +49-241-80 92642.

(1) Pulham, R. J.; Hubberstey, P.; Down, M. G.; Thunder, A. E. *J. Nucl. Mater. A* **1979**, *85−86*, 299.
(2) Vannerberg, N.-G. *Acta Chem. Scand.* **1962**, *16*, 2263.
(3) Liu, X.; Krott, M.; Müller, P.; Hu, C.; Lueken, H.; Dronskowski, R. *Inorg. Chem.* **2005**, *44*, 3001.
(4) Liu, X.; Wankeu, M. A.; Lueken, H.; Dronskowski, R. *Z. Naturforsch.* **2005**, *60b*, 593.
(5) Krott, M.; Liu, X.; Fokwa, B. P. T.; Speldrich, M.; Lueken, H.; Dronskowski, R. *Inorg. Chem.* **2007**, *46*, 2204.
(6) Liu, X.; Stork, L.; Speldrich, M.; Lueken, H.; Dronskowski, R. *Chem. Eur. J.* **2009**, *15*, 1558.
(7) Liu, X.; Decker, A.; Schmitz, D.; Dronskowski, R. *Z. Anorg. Allg. Chem.* **2000**, *626*, 103.
(8) Dronskowski, R. *Z. Naturforsch.* **1995**, *50b*, 1245.
(9) Strid, K. G.; Vannerberg, N. G. *Acta Chem. Scand.* **1966**, *20*, 1064.
(10) Wissmann, B. Ph.D. Dissertation, Universität Tübingen, Germany, 2001.

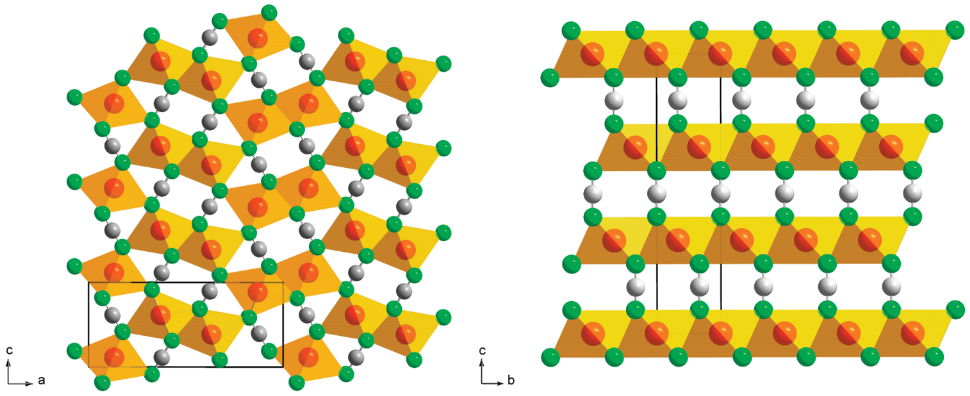

Figure 1. Polyhedral projections of the crystal structures of α-SrNCN (left) and β-SrNCN (right) with the SrN_6 octahedra given in orange, Sr atoms in red, N atoms in green, and C atoms in gray.

but the remaining two are flipped against the other four. This results in corrugated layers of edge-sharing octahedra which also engage in corner sharing.

We have recently found a new synthetic route leading to single crystals of α- and β-SrNCN using a reaction between NaCN, NaN_3, and SrI_2 in sealed tantalum containers[11,12] at different temperatures. We now report on further synthetic improvements such as a novel low-temperature route, structural investigations, total-energy and phonon calculations, as well as DSC measurements, targeted at the thermochemical ranking of the two polymorphs.

Experimental Section

Three synthetic techniques were used for the temperature-dependent preparations of the two SrNCN polymorphs.

Synthesis No. 1. SrI_2 (99.99%) was purchased from Aldrich, and ZnNCN was freshly prepared. To do so, 1 equiv of ZnI_2 (99%, Merck) was dissolved in demineralized water, and 1 equiv of H_2NCN (98%, Aldrich), also dissolved in demineralized water, was added to the well-stirred solution which was further stirred for 3 h. The white precipitate was filtered, washed with water and ethanol, and dried in high vacuum at 120 °C for 12 h.

Unless otherwise noted, all following manipulations were performed in a glovebox under a purified argon atmosphere. Note that tantalum containers are mandatory because the alkaline-earth iodides react with oxygen, water, glass and also ceramic containers to form very stable hydroxides and oxides. Because of the sensitivity against humidity and oxygen, the metal containers and the silica tubes were heated at 1273 K in vacuum for 12 h and then transferred into the glovebox. The starting materials (1 mmol each) were ground together in an agate mortar and placed in a semiopen Ta container. The container was placed into a silica tube, and the silica tube was closed with a glass valve. The tube was placed upright into a furnace and heated up to the reaction temperature within 24 h. The temperature was held for further 48 h, and then the furnace was cooled at 30 °C per hour to room temperature. During the entire duration of the reaction the tube was evacuated to 5×10^{-6} mbar. The product always appeared as a white crystalline powder. The metathesis reactions thus correspond to

$$SrI_2 + ZnNCN \rightarrow \alpha/\beta\text{-}SrNCN + ZnI_2$$

and only differ in the chosen temperatures (973 and 843 K). The phase ZnI_2 is achieved as a volatile side-product which is removed during the reaction to maximize the yield.

Synthesis No. 2. SrI_2 (99.99%) and CsN_3 (99.99%) were purchased from Aldrich. CsCN was prepared as described in the literature.[13] The preparation is identical with the one mentioned above, with the exception that the tube is not evacuated upon heating. The reactions follow the equation

$$SrI_2 + CsCN + CsN_3 \rightarrow \alpha/\beta\text{-}SrNCN + 2CsI + N_2$$

and yield CsI as a side-product which must be removed in a subsequent step. Thus, the raw product was ground with 2 equiv of CsBr and heated under vacuo at 923 K for 12 h. The CsBr·CsI mixture then evaporates and reappears at the cold part of the tube.

Whenever the above reaction was performed in sealed (instead of open) Ta containers at 843 K, the presence of elemental nitrogen caused a further pressure dependence of SrNCN formation (see below).

Synthesis No. 3. An entirely new method to synthesize both polymorphs of SrNCN utilizes very low temperatures. Elemental strontium (99.99%, Aldrich) and H_2NCN (98%, Aldrich) in a molar ratio of 1:1 were dissolved in liquid ammonia at 195 K. The resulting blue solution was allowed to stir for 2 h before the liquid ammonia was evaporated. The remaining white powder was evacuated and heated to 773 K in a semiopen Ta container to increase crystallization and remove any remaining ammonia. The product was characterized as β-SrNCN on the basis of X-ray diffraction (XRD). When the resulting white powder was heated up to 1073 K, the product changed into α-SrNCN. The reaction follows the simplest possible equation

$$Sr + H_2NCN \rightarrow \alpha/\beta\text{-}SrNCN + H_2$$

Characterization

X-ray Studies. X-ray analysis was performed on a Huber G 670 Guinier powder diffractometer with strictly monochromatized Cu–Kα_1 radiation. All measurements were performed in an evacuated flat sample-holder to protect the products from oxygen and moisture. Rietveld refinements, depicted in Figure 2, were carried out with the programs FullProf and WinPlotr.[14,15] Numerical details can be found in Table 1.

---

[11] Liao, W. Ph.D. Dissertation, RWTH Aachen University, Germany, 2005.

[12] Liao, W.; Dronskowski, R. *Acta Crystallogr.* **2004**, *E60*, i124.

[13] Markley, T. J.; Toby, B. H.; Pearlstein, R. M.; Ramprasad, D. *Inorg. Chem.* **1997**, *36*, 3376.

[14] Rodriguez-Carvajal, J. *Physica B.* **1993**, *192*, 55.

[15] Roisnel, T.; Rodriguez-Carvajal, J. *WinPLOTR: a Windows tool for powder diffraction patterns analysis, Materials Science Forum*; Proceedings of the Seventh European Powder Diffraction Conference (EPDIC 7) 2000; Delhez, R., Mittenmeijer, E. J., Eds.; p 118.

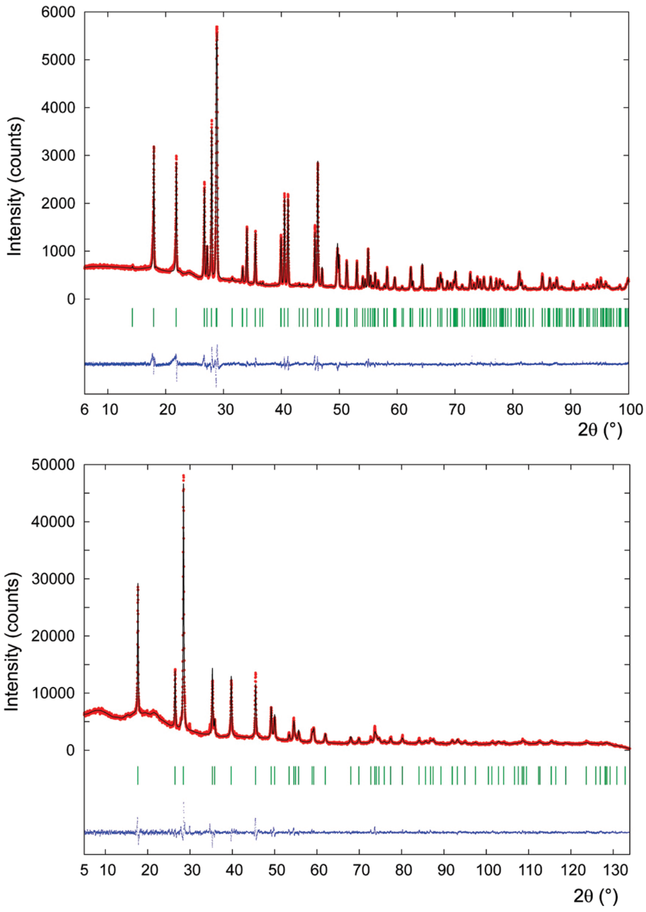

Figure 2. Powder XRD patterns of α-SrNCN (top) and *β*-SrNCN (bottom).

Table 1. Results of the Rietveld Refinements of α- and *β*-SrNCN

	α-SrNCN	*β*-SrNCN
space group, No., *Z*	*Pnma*, 62, 4	$R\bar{3}m$, 166, 3
lattice parameter		
a (Å)	12.4089(10)	3.9827(1)
b (Å)	3.9598(2)	*a*
c (Å)	5.3878(3)	15.0260(1)
calculated density, ($g \cdot cm^{-3}$)	3.20	3.08
molar volume ($cm^3 \cdot mol^{-1}$)	39.888	41.442
R_{Bragg}	0.059	0.042
R_p	0.041	0.058

The results of the structural refinement of the two polymorphs are in good agreement with the literature. Both lattice parameters and averaged bond lengths match, within three standard deviations, with the details from preceding contributions. Berger and Schnick[16] reported averaged *d*(Sr−N) = 2.637(6) Å and *d*(N=C) = 1.225(11) Å for α-SrNCN, which compare well with our results: *d*(Sr−N) = 2.644(4) Å and *d*(N=C) = 1.203(8) Å. For *β*-SrNCN, Liao and Dronskowski[12] specified *d*(Sr−N) = 2.623(2) Å and *d*(N=C) = 1.232(5) Å, in good agreement with this work which arrives at *d*(Sr−N) = 2.621(2) Å and *d*(N=C) = 1.246(5) Å.

In addition, temperature-dependent X-ray studies were performed to precisely determine the temperature of the *β*-to-α phase transformation. The measurements were done using a Huber G644 Guinier powder diffractometer equipped with a resistance heater and a linear position-sensitive detector.

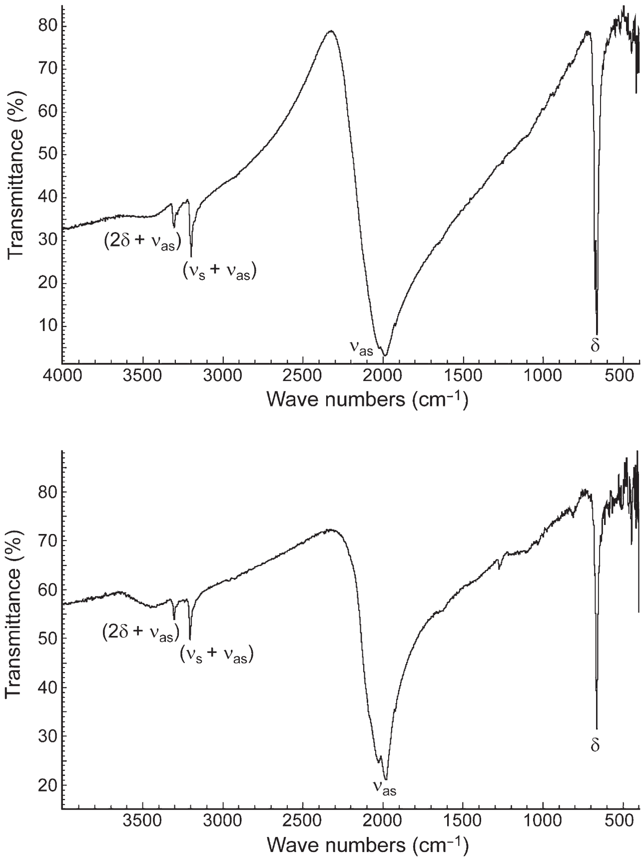

Figure 3. IR spectra of α-SrNCN (top) and *β*-SrNCN (bottom).

Infrared Spectroscopy. Infrared spectra (Figure 3) were recorded at room temperature using a Fourier transform Avatar 360 ESP spectrometer (Nicolet) in the range 400−4000 cm^{-1}. To do so, the samples were dispersed in strictly anhydrous KBr and pressed into pellets (Ø = 1.3 cm).

Differential Scanning Calorimetry (DSC). Differential scanning calorimetric measurements were performed with the aid of a DSC 404 apparatus (Netzsch) in the temperature range between 313−1023 K at a heating rate of 50 K/min. To shield the sample (9 mg) against oxidation, it was kept under a protective argon atmosphere throughout the measurement.

Theoretical Calculations

Density functional theory (DFT) total-energy calculations were performed using plane waves and pseudopotentials by means of the computer program VASP (Vienna *Ab Initio* Simulation Package)[17,18] employing the generalized-gradient approximation (GGA) of PBE type[19] and the projector-augmented wave (PAW) method;[20] the cutoff energy was set to 500 eV. Both unit cells of α- and *β*-SrNCN were allowed to

---

(16) Berger, U.; Schnick, W. *J. Alloys Compd.* **1994**, *206*, 179.

(17) Kresse, G.; Furthmüller, J. *Comput. Mater. Sci.* **1996**, *6*, 15. Kresse, G.; Furthmüller, J. *Phys. Rev. B* **1996**, *55*, 11169.

(18) Kresse, G.; Hafner, J. *Phys. Rev. B* **1993**, *47*, 558. Kresse, G.; Hafner, J. *Phys. Rev.B* **1994**, *49*, 14251.

(19) Perdew, J. P.; Burke, K.; Ernzerhof, M. *Phys. Rev. Lett.* **1996**, *77*, 3865.

(20) Blöchl, P. E. *Phys. Rev. B* **1994**, *50*, 17953.

change in volume and shape, and all atomic positions were allowed to relax, too. Because of the expected small total-energy differences the convergence criterion of the electronic structure calculation was chosen as 10^{-6} eV. The bulk modules were obtained by fitting a Murnaghan-type equation of state to the energy−volume data in the proximity of the equilibrium volumes. In addition, theoretical phonon densities-of-states and spectra were calculated using the quasi-harmonic approximation by means of the FROPHO utility[21] together with VASP, followed by subsequent thermodynamic calculations[22] targeted at theoretical Gibbs free energies.

Results and Discussion

In comparison with the preceding synthetic approach,[10] the present solid-state routes yield both phases of strontium carbodiimide at 30−200 K lower reaction temperatures. While α-SrNCN can be prepared phase-pure using all three methods, the synthesis of β-SrNCN is accompanied by side-products in the case of the solid-state routes, in part explainable by the low transition temperature of β-SrNCN to α-SrNCN. Within synthesis no. 1, the low reaction temperature results in an unknown side-product whose scattering contribution is on the order of 15% if based on integrated X-ray intensities. Unfortunately, we have been unable to separate this unknown phase from β-SrNCN. Within synthesis no. 2, the removal of CsI is achievable at 923 K which is slightly above the first transition temperature such that this approach must result in a mixture of both phases. Lower temperatures, however, lead to an incomplete CsI removal. Fortunately enough, synthesis no. 3 gives the best results, leading to phase-pure β-SrNCN (Figure 2) on the basis of XRD.

In accordance with the XRD data, infrared measurements indicate that the carbodiimide structure is present. Both IR spectra (Figure 3) show the characteristic frequency sequence of the linear three-atoms group with $D_{\infty h}$ symmetry, typical for the carbodiimide unit. For α-SrNCN (top) the ν_{as} vibration occurs at 1987/2024 cm^{-1} and the δ vibration at 676/664 cm^{-1}. For β-SrNCN (bottom) the ν_{as} vibration is observed at 1981/2028 cm^{-1} and the δ vibration at 663 cm^{-1}. These experimental frequencies are in very good agreement with both the literature[10,16] and also those that have been calculated on the basis of DFT and the quasi-harmonic approximation. According to the theoretical phonon spectra depicted in Figure 4 the asymmetric carbodiimide vibration can be found at 2010 cm^{-1} while the δ vibration is located at 650 cm^{-1} for both structures. In addition, the Raman-active but IR-inactive symmetric vibration is visible in the theoretical phonon spectra, namely, at 1260 cm^{-1}.

Furthermore, the first-principles phonons give a first conclusive hint concerning the relative thermodynamical stabilities of both phases. Only for the case of α-SrNCN (top) the calculated spectrum contains negative [Note that the calculations yield, in fact, imaginary frequencies which are typically displayed in negative form.] low-energy frequencies (see inset) while none such are found for β-SrNCN (bottom). Thus, the structure of α-SrNCN must be considered an unstable transition state which will decay into the stable β-SrNCN ground-state structure, in harmony with the fact that the α-phase occurs at higher and the β-phase at lower temperatures.

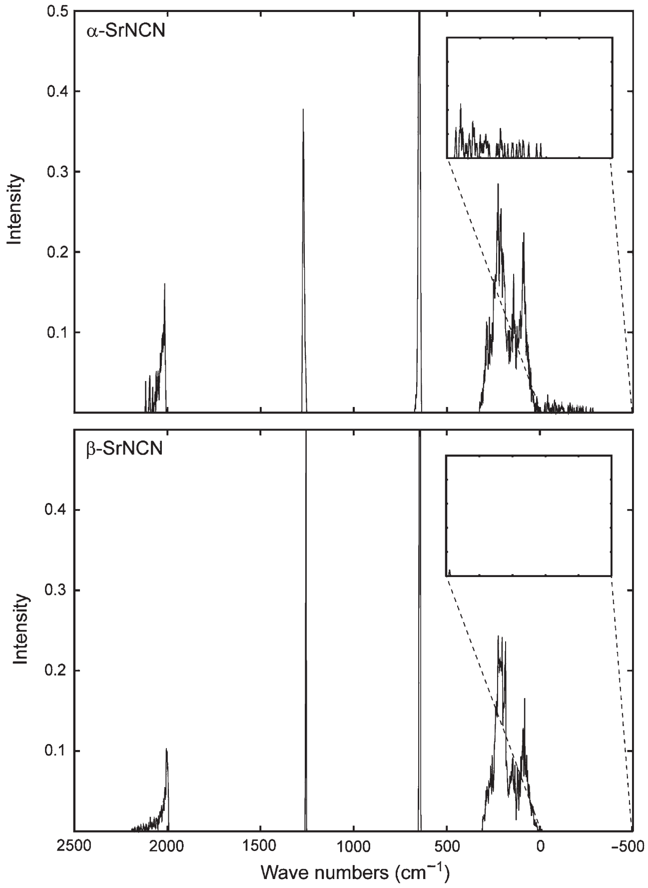

Figure 4. Theoretical (DFT-GGA) phonon spectra of α-SrNCN (top) and β-SrNCN (bottom) as calculated using the quasi-harmonic approximation.

Figure 5 displays a temperature-dependent X-ray pattern of β-SrNCN starting at room temperature. There is an obvious phase transition toward α-SrNCN beyond a temperature of about 900 K which, surprisingly, occurs 280 K lower than the one given in ref 10. Nonetheless, we note that the latter was not determined using pure SrNCN but, instead, using a reaction mixture. A closer look into our X-ray data (Figure 5) also yields that the phase transformation seemingly occurs through *two* distinct steps: there is the new (201) reflection of α-SrNCN which defines, first, a transformation temperature of 920 ± 20 K (lower dashed horizontal line). In addition, there is another change in intensities, at approximately 985 ± 15 K (upper dashed horizontal line), with an additional but weaker reflection around 25.5° in 2Θ.

The temperature range of the above two intensity changes is in good agreement with the first theoretical (GGA density-functional) estimate (see below). In addition, it is worthwhile noting that the β-to-α phase transition is irreversible in the XRD experiment because α-SrNCN does not recrystallize into β-SrNCN upon cooling once it has been found. Such a transformation would require the reorientation of two of the six coordination carbodiimide groups

---

(21) Togo, A. *FROPHO: a tool to compute phonon band structures and thermal properties of solids*; RWTH Aachen University: Aachen, Germany, 2008. Available at: http://fropho.sourceforge.net. Togo, A.; Oba, F.; Tanaka, I. *Phys. Rev. B* **2008**, *78*, 134106.

(22) Stoffel, R., dissertation under preparation, RWTH Aachen University.

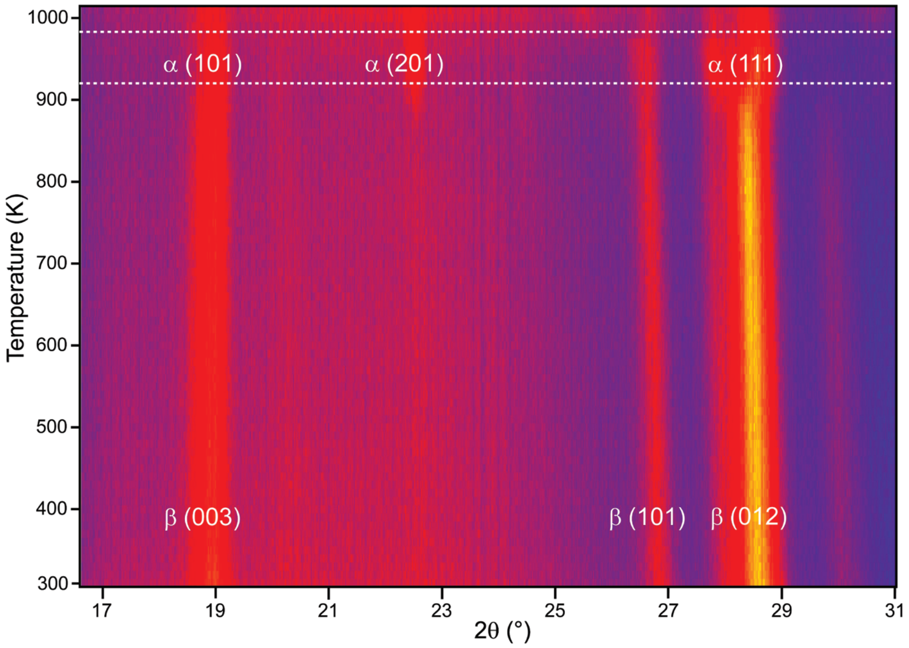

Figure 5. Temperature-dependent powder XRD pattern of SrNCN starting from room temperature (bottom) to slightly above 1000 K (top). High and low absolute intensities are displayed in yellow and blue, respectively. Note the two distinct intensity changes around 920 ± 20 K (lower dashed horizontal line) and 985 ± 15 K (upper line).

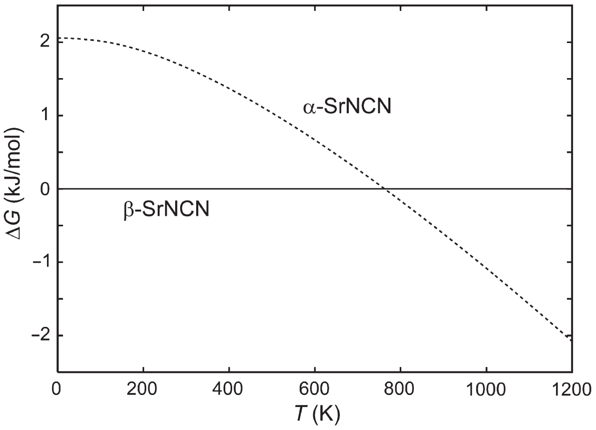

Figure 6. Theoretical Gibbs free energy−temperature diagram for α-SrNCN and β-SrNCN as calculated by DFG-GGA and the quasi-harmonic approximation.

Table 2. DFT-GGA Total-Energy Results for α- and β-SrNCN

	ΔE (kJ/mol)	ΔV (cm^3/mol)	B_0 (GPa)	B_0'
α-SrNCN (*Pnma*)	2.0	−1.19	53.4	4.17
β-SrNCN ($R\bar{3}m$)	0.0	0.00	54.5	3.83

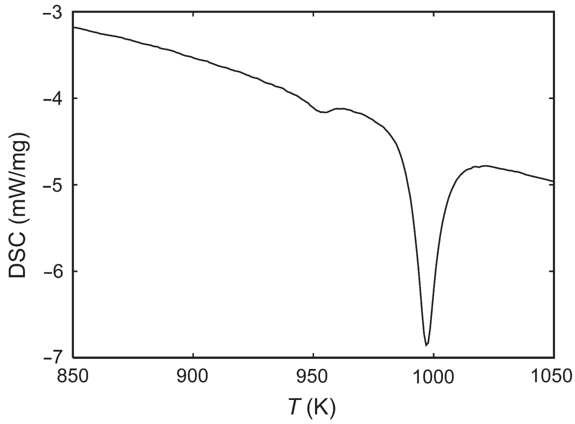

Figure 7. DSC of β-SrNCN in going from T = 850−1050 K; see also text.

together with bond breaking and formation (see Figure 1 and structural discussion above), not just a simple bond-length adjustment.

If synthesis no. 2 is carried out in a sealed tantalum container at 823 K, the reaction results in a *mixture* of the α- and β-phase, a result which is easily explainable by their different molar volumes V_{mol} and Le Chatelier's principle: Because V_{mol} of α-SrNCN is smaller by almost 1.2 cm^3/mol, the formation of this high-temperature phase may be enforced by a moderate nitrogen pressure (about 6 bar) at lower temperatures already, as is observed experimentally.

The results of the DFT phonon calculations corroborate the prior experimental findings, as seen from Figure 6 which displays a theoretical Gibbs free energy−temperature diagram. The theoretical T = 0 K data already reveal (Table 2) that β-SrNCN is the thermochemically favored phase, but only by a mere 2 kJ/mol. Upon increasing the temperature above 760 K (Figure 6), α-SrNCN will eventually be thermodynamically favored. As said before, the difference between the experimental transition temperature (beyond 900 K) and the theoretically calculated one (760 K) is more than 140 K which corresponds to an error of only 1 kJ/mol using the GGA, which is quite remarkable. In addition, the larger density of α-SrNCN (Table 1) favors this phase's existence at higher pressures, as explained above. The bulk moduli arrive at almost the same value (about 54 GPa, Table 2), with β-SrNCN being slightly stiffer.

In addition, DSC (Figure 7) reveals that β-SrNCN changes into α-SrNCN at higher temperatures in an endothermic manner, as expected for this kind of transformation. Puzzlingly enough, and in good agreement with the XRD measurement, one first observes a very small endothermic peak, on the order of 0.3 kJ/mol, close to 950 K. In addition, one finds a much larger endothermic peak on the order of 5.9 kJ/mol at about 995 K, which also mirrors the preceding XRD observation. Thus, β- and α-SrNCN energetically differ from each other by roughly 6 kJ/mol, and this is in good agreement with the DFT result for absolute zero temperature (ca. 2 kJ/mol) taking into account the presently possible accuracy of first-principles theory.

Acknowledgment. It is a pleasure to thank the Deutsche Forschungsgemeinschaft for financial support. We also thank the computing center of RWTH Aachen for having provided their computing resources.